Absorption of CO_2 laser radiation in an exploded lithium wire plasma*†

James C. DeBoo‡ and David R. Bach

Nuclear Engineering Department, The University of Michigan, Ann Arbor, Michigan 48105
(Received 15 October 1973; in final form 11 October 1974)

An absorption experiment was performed with a pulsed TEA CO_2 laser incident upon a partially ionized plasma created by exploding a 0.0025-cm-diam lithium wire in vacuum. Stark broadening of the Li I 6104-Å line and line intensity ratios of the same line to the Li II 5485−Å line were used to extract the density and temperature from time-resolved emission spectra. The neutral density was found from absorption measurements at 6328 Å and compared well with particle conservation calculations. In order to explain the strong observed absorption of both 10.6-μ and 6328-Å radiation, the plasma was assumed to consist of a hot peripheral region containing electrons and singly ionized lithium ions and a colder central region of excited neutrals. The model was supported by computer calculations and spectroscopic observations. Absorption of the 10.6-μ radiation was dominated by inverse bremsstrahlung in the field of ions and in the presence of neutrals.

PACS numbers: 52.25.P, 52.70.K, 52.80.

I. INTRODUCTION

Progress toward laser-driven fusion has stimulated considerable interest in laser radiation absorption in dense plasmas.[1–3] It is believed that at high laser intensities plasma instabilities are generated.[4–7] Since these processes may be responsible for strong absorption (pellet heating) or strong reflection (no heating), they are under intense study.[8–11] In this investigation, however, the laser intensity was well below the calculated thresholds necessary for the production of these plasma instabilities.

Laser absorption and heating experiments have been performed previously,[12–17] but the electron density has been typically far less than the critical density. The purpose of this investigation was to study the photon interaction in a plasma with an electron density near the critical density. The major absorption mechanism in this case was expected to be inverse bremsstrahlung (IB).

An exploded wire system provided a simple means of achieving a high-density low-temperature plasma. The radiation source was a pulsed CO_2 laser. As an aid in determining the neutral density, absorption of 6328-Å radiation was also measured. Strong absorption was observed at both wavelengths, and in order to explain the absorption consistently, a qualitative model for the electron and neutral density spatial distributions was postulated and supported by spectroscopic observations. It was assumed that the plasma consisted of a hot peripheral region predominantly containing electrons and singly ionized lithium ions, and a colder central region containing mainly high-density excited neutrals. Absorption of 10.6-μ radiation was dominated by inverse bremsstrahlung in the field of ions and in the presence of neutrals.

In Sec. II, theoretical expressions for the pertinent absorption coefficients are given. These include IB in the field of ions, IB in the presence of ground- and excited-state neutrals, and photoionization.

A description of the experiment is given in Sec. III. Absorption data are given in Sec. IV which includes a discussion of the line ratio and Stark broadening methods used to determine the electron temperatures and densities. Qualitative plasma density profiles are also discussed in Sec. IV.

II. THEORY

Electromagnetic radiation may be reflected, refracted, scattered, or absorbed in passing through a system of free electrons, ions, and neutral atoms. Before proceeding with the discussion of absorption, some remarks concerning the other processes will be made. Since the CO_2 laser frequency was only a factor of 2 larger than the electron plasma frequency, it was necessary to consider carefully the influence of reflection and refraction on the absorption measurements.

The laser intensity was well below the threshold intensity for instability generation, consequently, strong anomalous reflection was not expected. An attempt was made to observe radiation reflected from the vacuum-plasma boundary. A beam splitter was placed on the optical axis between the laser and the lens that focused the radiation onto the plasma. The reflected radiation coming back through the focusing lens was deflected 90° by the beam splitter into a detector. No signal was observed, indicating the reflected energy at the detector was less than 1 mJ, the minimum detectable energy of the detector. Taking the geometry and beam splitter reflectivity into account, the reflected energy was therefore determined to be less than 20% of the incident energy. A second estimate was made by calculating the Fresnel reflection from an infinite density gradient at the vacuum-plasma boundary, and yielded a total reflected energy of less than 1% of the incident energy. This is believed to be a more realistic result and is consistent with the reflection of ruby laser light observed from an exploded wire plasma[18] when the wavelength difference and geometry were taken into account.

Refraction from density gradients within the plasma was estimated by assuming several different density profiles and calculating the maximum refraction angle for each profile. The largest of these angles ($\approx 23°$) was then used to choose and place a collecting lens. Verification that all transmitted light was collected was difficult to establish experimentally. However, the viewing angle of the collecting lens was conservatively chosen to be 27°.

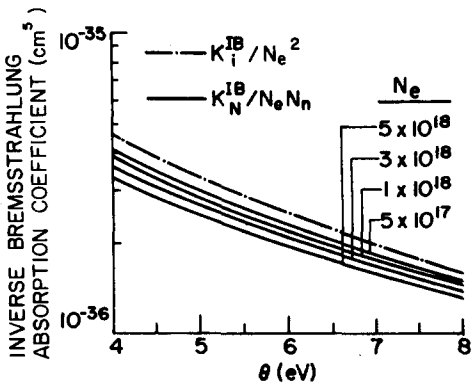

FIG. 1. Absorption coefficients of inverse bremsstrahlung in the field of ions and neutral atoms as a function of temperature and density ($\lambda = 10.6\ \mu$).

Beam attenuation due to Thomson scattering was negligible since the Thomson scattering cross section is much smaller than the absorption cross sections of interest. Negative lithium ions were not expected to be present since the electron affinity for lithium is about 0.6 eV[19] and plasma temperatures were 5—6 eV.

The absorption mechanisms relevant to this investigation and discussed in this section are IB in the field of ions (ion IB), IB in the presence of ground-state and excited neutrals (neutral IB), and photoionization. Absorption coefficients for the first two processes were calculated for 10.6 μ. Photoionization was found to be negligible at 10.6 μ, but was the dominant absorption process at 6328 Å and was used as an aid in estimating the neutral density in the plasma.

A. Ion IB absorption coefficient

The expression[20] for the absorption coefficient for ion IB, K_i^{IB}, is well known and is

$$K_i^{IB} = \frac{4}{3}\left(\frac{2\pi}{3\theta}\right)^{1/2}\frac{e^6}{hcm_e^{3/2}}\frac{g_{ff}}{\nu^3}Z^2N_eN_i[1-\exp(-h\nu/\theta)], \tag{1}$$

where Z is the degree of ionization, N_e and N_i are electron and ion densities, $\theta = kT$ is the electron temperature, g_{ff} is the free-free Gaunt factor, and $1-\exp(-h\nu/\theta)$ is the correction term for induced emission. The values of g_{ff} as functions of $h\nu$ and θ were taken from the tables of Karzas and Latter.[21]

For 10.6-μ radiation, the photon energy $h\nu = 0.117$ eV. Since the typical plasma temperatures were about 5 eV, $h\nu \ll \theta$ and Eq. (1) becomes

$$K_i^{IB} = 3.71\times10^{-35}N_e^2/\theta^{3/2} \tag{2}$$

where the dominant degree of ionization was assumed to be unity. The absorption coefficient is shown in Fig. 1 as a function of temperature. The increase in path length through the plasma due to the plasma index of refraction, $n_i = (1-N_e/N_c)^{1/2}$, where N_c is the critical electron density, was taken into account when a measured absorption coefficient was compared with Eq. (2).

B. Neutral IB absorption coefficient

In a partially ionized plasma at about 5 eV, a significant number of neutral atoms are in highly excited states and must be included in the calculation of the neutral IB absorption. Tsai, Akcasu, and Osborn[22] treated this case for plasma temperatures in which a significant fraction of the neutrals are in highly excited states. Oktay[12] applied the theory for 6328-Å radiation to neutrals in a lithium plasma. The neutral IB absorption coefficient for 10.6-μ radiation is

$$K_N^{IB} = 1.15\times10^{-36}N_nN_e\theta^{-5/2}\sum_{n=2}^{n^*}g_{nn}N(n)/N_n, \tag{3}$$

where again it was assumed that $h\nu \ll \theta$, N_n is the total neutral density, $N(n)$ is the number density in the nth energy state, g_{nn} is related to the collision cross section of electrons with neutral atoms in the nth excited state, and n^* is the highest state in which an electron is still bound. For $n > n^*$, the atom was assumed to be ionized. The summation in Eq. (3) begins at $n = 2$, the principal quantum number of the ground state of neutral lithium.

Tsai, Oktay, and Akcasu[23] calculated g_{22}, g_{33}, and $g_{\infty\infty}$ as functions of photon energy for various temperatures. These three values of g_{nn} were determined for a

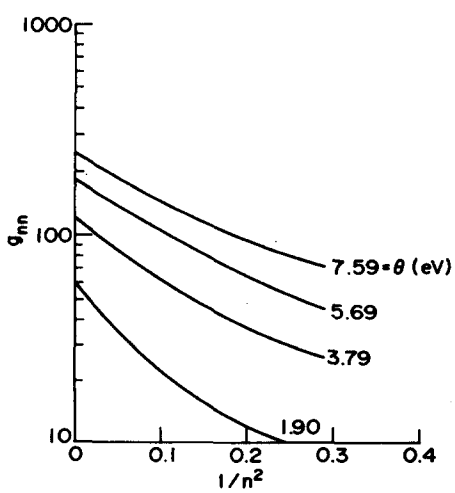

FIG. 2. g_{nn} versus $1/n^2$ for $h\nu = 0.117$ eV.

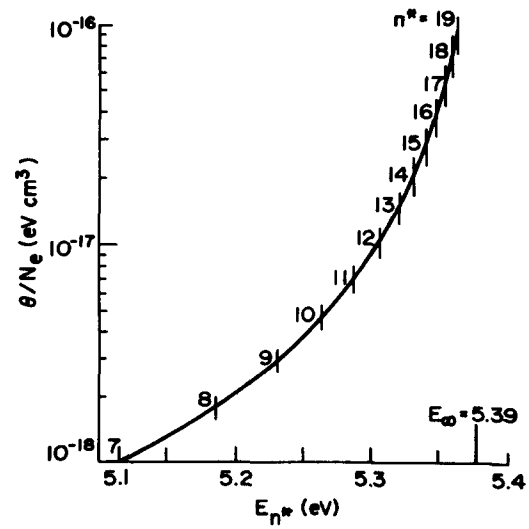

FIG. 3. θ/N_e versus E_{n^*}.

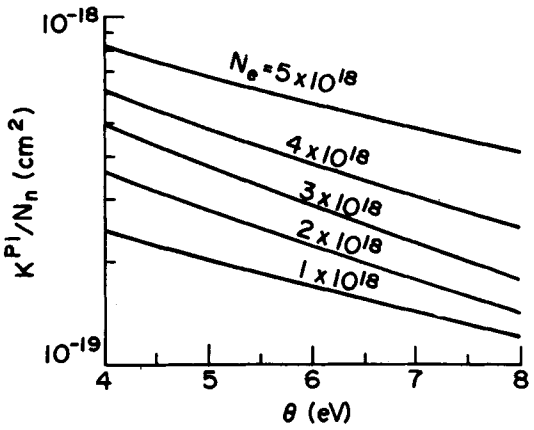

FIG. 4. Absorption coefficient for photoionization of neutrals as a function of temperature and density ($\lambda = 6328$ Å).

photon energy of 0.117 eV at several different temperatures and were plotted as a function of $1/n^2$. A smooth curve (Fig. 2) was drawn between the points and all other values of g_{nn} were determined from this curve.

The choice of n^* was based upon the calculated reduction in ionization energy, ΔE_∞, of the neutral atom. The principal quantum number of the highest energy level existing below the reduced ionization potential was chosen to be n^*. The criterion is

$$E_{n^*} \leq E_\infty - \Delta E_\infty. \tag{4}$$

The expression by Griem[24] was used to determine ΔE_∞. A plot of θ/N_e versus E_{n^*} is shown in Fig. 3 and shows the n^* associated with each energy level.

The fraction of neutrals in the nth excited state can be written

$$N(n)/N_n = g_n \exp(-E_n/\theta)[U(\theta)]^{-1}, \tag{5}$$

where g_n is the statistical weight of the nth excited state. The neutral lithium partition function, $U(\theta)$, was calculated as a function of θ. Although $K_i^{IB} \propto \theta^{-3/2}$ and $K_N^{IB} \propto \theta^{-5/2}$, the dependence of g_{nn} and $N(n)/N_n$ on temperature result in the approximate equality of K_i^{IB} and K_N^{IB} for temperatures above a few eV and for equal neutral and electron densities.

C. Photoionization

Wheeler and Fielding[25] have shown that, at 10.6 μ, the ratio of the photoionization absorption coefficient to the ion IB absorption coefficient is

$$\frac{K^{PI}}{K_i^{IB}} \approx \frac{h\nu/\theta}{g_{tt}}. \tag{6}$$

For a temperature of 5 eV, the ratio is about 10^{-2}. Hence, the absorption of 10.6-μ radiation due to photoionization was expected to be negligible in this experiment.

Oktay[12] found that photoionization of excited neutrals by 6328-Å radiation in an exploded lithium wire plasma was the dominant absorption mechanism. The absorption coefficient is

$$K^{PI} = \frac{64\alpha a_0^2 \pi}{3^{3/2}} \left(\frac{E_H}{h\nu}\right)^3 N_n \sum_{n=k}^{n^*} g_{bf} n^{-5} \frac{N(n)}{N_n}, \tag{7}$$

where α is the fine structure constant, a_0 is the first Bohr radius, and E_H is the Rydberg constant. The induced emission term was neglected and the bound-free Gaunt factor, g_{bf}, is approximately unity. The $n = k$ is the lowest energy level from which an atom may be ionized by the absorption of a 1.96-eV (6328-Å) photon. For lithium, the summation begins at $k = 3p$. The photoionization absorption cross section, K^{PI}/N_n, is plotted in Fig. 4 for temperatures between 4 and 8 eV and for several electron densities. The measurement of K^{PI} was used to determine the neutral density.

III. EXPERIMENTAL APPARATUS

A schematic diagram of the apparatus is shown in Fig. 5. A pin-type TEA CO_2 laser was used. A 0.05-μF capacitor, charged to 30 kV, was discharged through three rows of 1000-Ω 1-W carbon resistors. The 2-cm-diam laser beam was focused to a 1.5-mm diam spot at the plasma by a 25-cm-focal-length germanium lens. A 98% reflecting mirror was placed at the rear of the laser cavity. The radiation passing through the rear reflector was monitored using a photon drag detector[26] and was calibrated relative to the main output power. The FWHM laser pulse energy was 0.2 J. This gives an intensity of 5.7×10^7 W/cm^2 at the plasma surface for a FWHM pulse width of 200 nsec. The transmitted refracted beam was collected by a large AR-coated Ge lens and focused onto a pyroelectric detector.[27]

The exploded wire system was the same as that described by Leonard.[18] Lithium was extruded and exploded at an ambient pressure of 5×10^{-5} Torr. The plasma was created by discharging a 13.9-μF capacitor, charged to 15 kV, through a 0.0025-cm-diam lithium wire. The discharge current waveform, monitored by a Rogowski coil, was typical of underdamped LRC circuits and had a typical initial peak of 10^5 A at 3.5 μsec. Although the strong current induced pinching in the plasma, the column remained cylindrically symmetric for the first 2.5 μsec, during which time the absorption measurements were made.

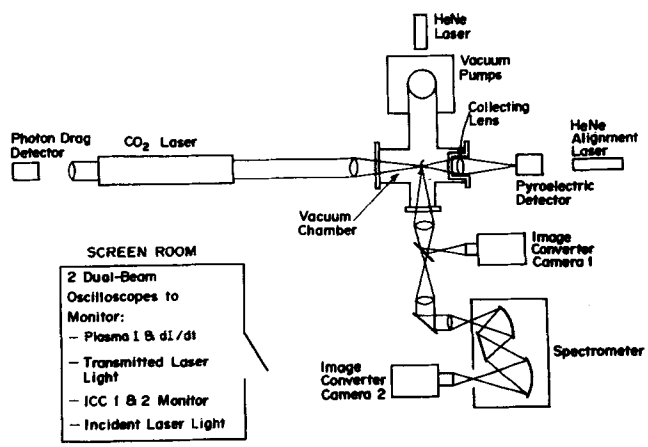

FIG. 5. Schematic diagram of experimental apparatus.

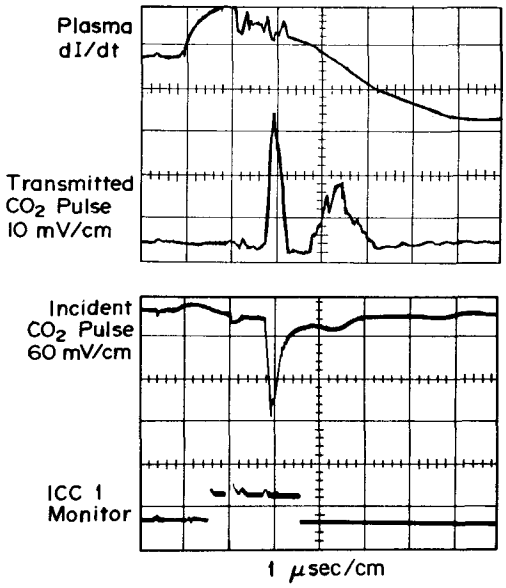

FIG. 6. Rogowski coil, pyroelectric detector, photon drag detector, and ICC 1 signals for data listed as entry 2 in Table I.

The diagnostic equipment consisted of two image converter cameras and an $f/6.3$ grating spectrometer. The first image converter camera, ICC 1, was equipped with a 2-μsec streak unit and was focused onto the laser-plasma interaction region. A 1-mm horizontal slit was placed in front of the camera photocathode. As this slit was vertically swept across the film, the time history of the oscillating plasma diameter was recorded.

The spectrometer and ICC 2 were used to record time-resolved plasma emission spectra from which the spatially averaged electron density and temperature were extracted. A 20-μsec streak unit was used on ICC 2 since the lithium line emission intensities were too low to allow faster streak rates to be used. The spectral time resolution was 0.4 μsec.

IV. ABSORPTION DATA AND ANALYSIS

A sample of raw data is given in Figs. 6 and 7. The current derivative and transmitted laser pulse are shown in the upper portion of Fig. 6 and the incident laser pulse and ICC 1 monitor are shown in the lower portion. Streak pictures of the plasma diameter (2-μsec streak) and emission spectra (20-μsec streak) are shown in Fig. 7. The laser pulse was incident on the plasma 2 μsec after the start of current flow. Since ICC 1 had a 2-μsec streak length, both streak units were triggered 0.7 μsec after current flow so that the laser pulse appears at 1.3 μsec on the 2-μsec streak picture in Fig. 7.

Perturbations in the current derivative trace roughly corresponded to pinches in the plasma column and resulted from inductive and resistive changes in the plasma. Plasma pinching resulted in increased emission and strong bursts of continuum, as shown in Fig. 7, indicating an increase in temperature. We were unable to measure the temperature and density during strong pinching because of the predominance of the continuum over the lithium emission lines at these times.

The small second peak in the incident laser pulse (Fig. 6) corresponds to the second peak in the transmitted laser pulse (note the different vertical scales) and was relatively unattenuated by the plasma, whereas the main pulse was strongly attenuated. The reason for this can be seen in Fig. 7. The time at which the main laser pulse was incident on the plasma is labeled t_L. The plasma disrupted 0.6 μsec after t_L, allowing the second laser pulse to pass. Hydrodynamic disruption of the plasma column was independent of t_L and usually occurred about 2.5 μsec after the discharge was initiated. Current continued to flow through the plasma for as long as 50 μsec.

Wavelength calibration lines appear at the beginning of the 20-μsec streak in Fig. 7. One important feature of each emission spectrum was the presence of a

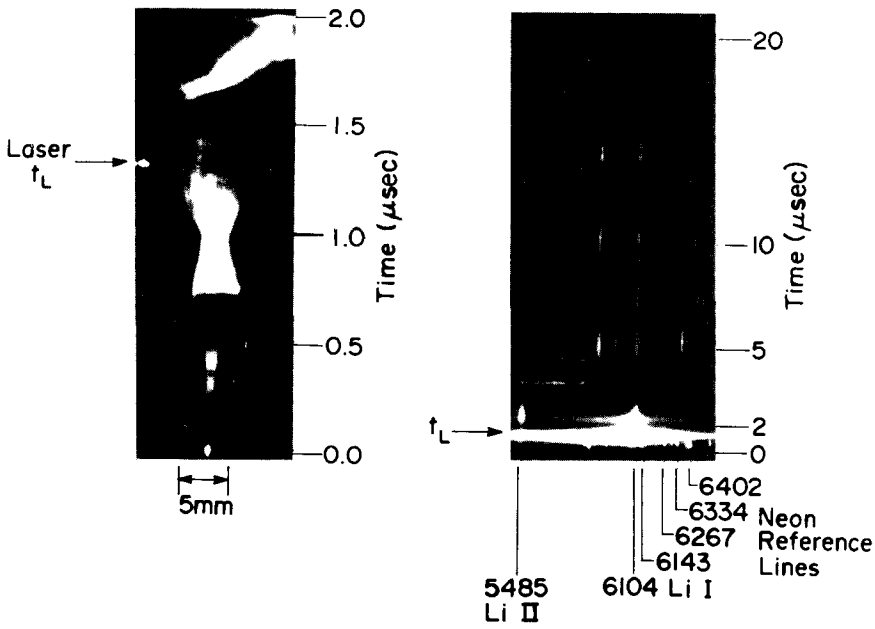

FIG. 7. Plasma streak and time-resolved emission spectra for data listed as entry 2 in Table I. The time of CO_2 laser incidence is t_L.

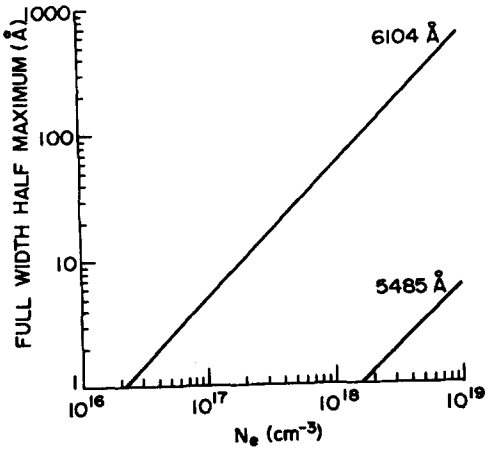

FIG. 8. Electron density versus the Stark broadening of two lithium lines.

clean lithium spectrum for the first 2 to 3 μsec, during which time the absorption measurements were made. Many carbon and copper impurity lines began to appear after this time.

A microdensitometer trace of the emission spectra provided measurements of linewidths and relative intensities which yielded the electron density and temperature. The Li I 6104-Å and Li II 5485-Å lines were used in the analysis because both were fairly well isolated and their intensities were well above the continuum except during strong plasma pinching when the analysis was impossible.

Stark broadening parameters taken from the tables of Griem[24] yielded the curves in Fig. 8. The linewidth versus electron density is given for two lithium lines. The 6104-Å linewidth was easily observable and was used to determine the electron density. The spectral resolution was ± 2.5 Å, giving a density resolution of $\pm 0.04 \times 10^{18}$ cm^{-3}.

The 5485-Å Li II line usually had a linewidth between 20 and 25 Å which yielded a rather unlikely electron density greater than the critical density of 10^{19} cm^{-3}. Since ion line broadening calculations[28] are generally less certain than neutral line broadening calculations, the 5485-Å Li II line data were not used to determine the electron density.

A sensitive temperature measurement was made by measuring the relative line intensity ratios from a subsequent, rather than the same, ionization state. The appropriate expression from Griem is

$$\frac{I'}{I} = \frac{\lambda^3 g' f'}{(\lambda')^3 g f} \left(4\pi^{3/2} a_0^3 E_H^{3/2}\right)^{-1} \frac{\theta^{3/2}}{N_e} \exp\left(-\frac{E_{u'} + E_\infty - E_u - \Delta E_\infty}{\theta}\right), \tag{8}$$

where the primed quantities refer to the higher ionization state, and E_u is the energy of the upper level of the transition. Equation (8) is based upon the validity of the Saha equation and complete LTE. As pointed out by Leonard,[18] LTE criteria are met for all neutral lithium levels and all levels above the ground state of Li II for electron densities of 10^{18} cm^{-3} and temperatures of a few eV. The 6104/5485 intensity ratio is plotted versus temperature in Fig. 9 for several electron densities. The spectral response of the image converter tube was included in the calibration of the relative intensities. Typical temperatures were between 5 and 6 eV, which agreed with Leonard's observations.

All plasma parameters were measured at the time the laser pulse was incident on the plasma, and this time was not changed with respect to the start of current flow (trigger jitter times were negligible). Since the plasma pinch dynamics were not repeatable, a significant shot-to-shot variation in plasma diameter and electron density was obtained.

A. Ion IB absorption

As a first step in the data analysis, the measured total absorption coefficient, K_T, for 10.6-μ radiation was compared to the calculated coefficient for inverse bremsstrahlung in the field of ions only, assuming a uniform electron density distribution. (Neutral IB absorption is considered in Sec. IV B.) The ion absorption coefficient, K_i^{IB}, was calculated from Eq. (2). Since plasma light entering the spectrometer was not spatially selected from any particular part of the plasma, the measured density and temperature were assumed to be average values for the entire plasma volume.

Table I is a list of the absorption data and the data shown in Figs. 6 and 7 are listed as entry 2. Absorption of 10.6-μ radiation ranged from 50 to 96%. The fraction of absorbed laser radiation is proportional to $1 - e^{-\beta}$ where $\beta \propto N_e^2 D_p / \theta^{3/2}$, in which D_p is the plasma

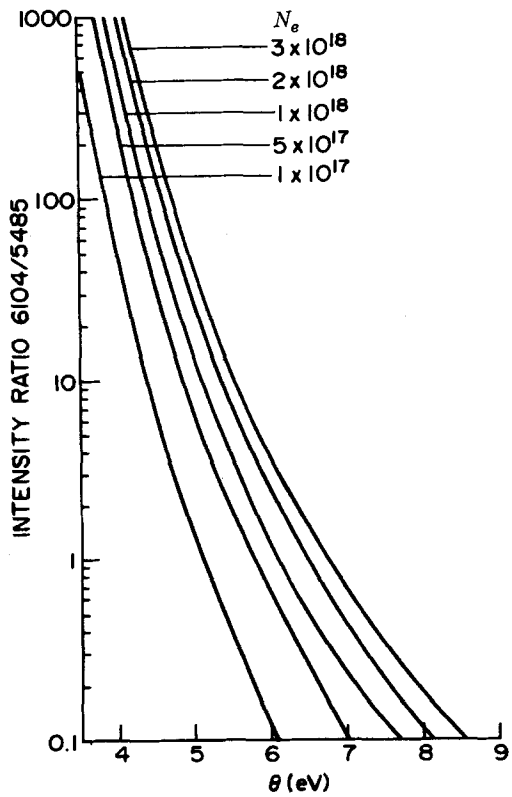

FIG. 9. Calculated intensity ratio of 6104/5485 as a function of temperature and density.

TABLE I. Summary of absorption data. D_p: plasma diameter; K_T: measured total absorption coefficient for 10.6 μ; K_i^{IB}: calculated ion IB absorption coefficient for 10.6 μ; A: measured 10.6-μ absorption (in percent).

N_e (cm^{-3})	θ (eV)	D_p (mm)	K_T (cm^{-1})	K_i^{IB} (cm^{-1})	A (%)
7.00×10^{17}	5.25	8.00	1.80	1.57	76.3
7.50×10^{17}	5.00	6.67	2.06	1.94	74.7
8.00×10^{17}	5.75	4.00	2.04	1.80	55.8
8.20×10^{17}	5.65	3.00	2.24	1.94	48.9
9.20×10^{17}	4.90	3.00	3.90	3.04	69.0
9.30×10^{17}	5.60	5.30	2.20	2.54	68.8
1.00×10^{18}	5.00	3.30	2.76	3.50	59.8
1.06×10^{18}	5.60	3.30	3.49	3.33	68.4
1.10×10^{18}	5.50	1.50	7.49	3.69	67.5
1.10×10^{18}	5.00	2.00	4.39	4.26	58.4
1.35×10^{18}	5.00	4.00	6.35	6.50	92.1
1.50×10^{18}	5.80	2.00	6.51	6.48	72.8
1.80×10^{18}	6.50	2.00	6.42	8.01	72.3
1.90×10^{18}	5.60	1.67	6.61	11.2	66.8
2.05×10^{18}	5.60	2.67	9.91	13.2	92.9
2.10×10^{18}	5.00	1.50	16.6	16.5	91.7
2.20×10^{18}	5.60	2.00	16.6	15.3	96.4
2.60×10^{18}	5.60	1.67	17.7	22.0	94.8

diameter. The rather large range in absorption was caused by shot-to-shot fluctuations in the plasma diameter and electron density. (The temperature remained about the same from shot to shot.) It should be noted that no plasma heating was observed due to laser absorption since the laser energy deposited in the plasma was considerably less than 1% of the plasma energy.

A comparison of K_T and K_i^{IB} is presented in Fig. 10. The error in K_T was reasonably small because of the small error in measuring each of the associated parameters. However, the error in calculating K_i^{IB} was rather large due in part to the squared density dependence and $\frac{3}{2}$ power temperature dependence. The errors in evaluating the density were dominated by theory, whereas the major error in estimating the temperature

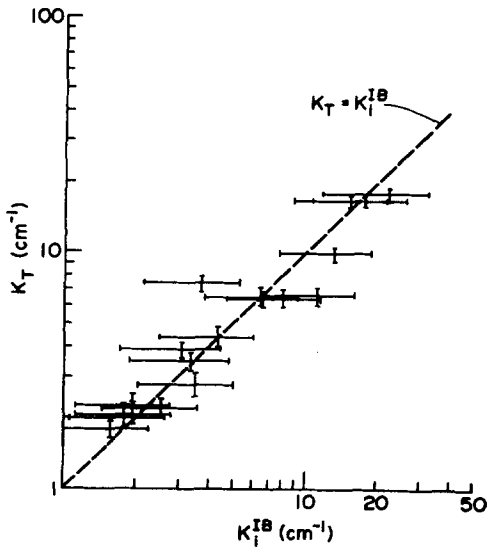

FIG. 10. Total measured absorption coefficient versus calculated coefficient for inverse bremsstrahlung in the field of ions ($\lambda = 10.6\ \mu$).

was experimental. Griem estimated a theoretical uncertainty of ≈15% in measuring the electron density using Stark broadening theory. The poor time resolution, 0.4 μsec, of the emission spectra was the major contribution to the 20% uncertainty in the temperature. Figure 11 tends to strengthen the temperature estimates, as it illustrates that all the measured absorption coefficients lie within a small temperature range about the estimated temperatures.

B. Neutral density consideration

As shown in Fig. 1, for $N_n \approx N_e$, the neutral IB and ion IB absorption coefficients are approximately equal for temperatures of a few eV and above. Since previous exploded lithium wire studies[12,18] had shown that the neutral density (≈10^{19} cm^{-3}) was typically larger than the electron density (≈10^{18} cm^{-3}), the agreement found here between the total absorption coefficient and that calculated for ion IB only, shown in Fig. 10, was puzzling. It was necessary to explain the apparently negligible neutral IB absorption of the 10.6-μ radiation.

A previous experiment[12] showed that absorption at 6328 Å was largely due to photoionization of neutrals in excited states. In order to determine the total neutral density and thereby determine K_N^{IB}, a simultaneous absorption measurement was made at 6328 Å and 10.6 μ. A cw HeNe laser was directed so as to intercept the plasma in the same region as the CO_2 laser beam. The HeNe laser intensity was recorded by ICC 2 after passing through the spectrometer. Figure 12 is a typical streak picture of the emission spectra and the HeNe radiation and shows that the 6328-Å laser line was strongly absorbed during the first few microseconds of the discharge. Reappearance of the line was attributed to decreasing neutral density and finally plasma disruption. In this example, the HeNe laser beam absorption was 82% at the time the CO_2 laser pulse was incident upon the plasma.

The plasma and CO_2 laser absorption data are listed as entry 12 in Table I. For this example $K_T^{6328} = 6.55$ cm^{-1} and was assumed to be equal to K^{PI}. The neutral density found from Fig. 4 was 3.6×10^{19} cm^{-3} which was

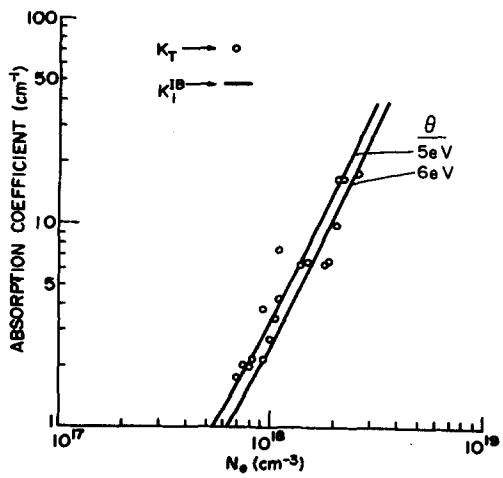

FIG. 11. Total measured absorption coefficient versus electron density. The two solid lines are the calculated ion IB absorption coefficient for temperatures of 5 and 6 eV.

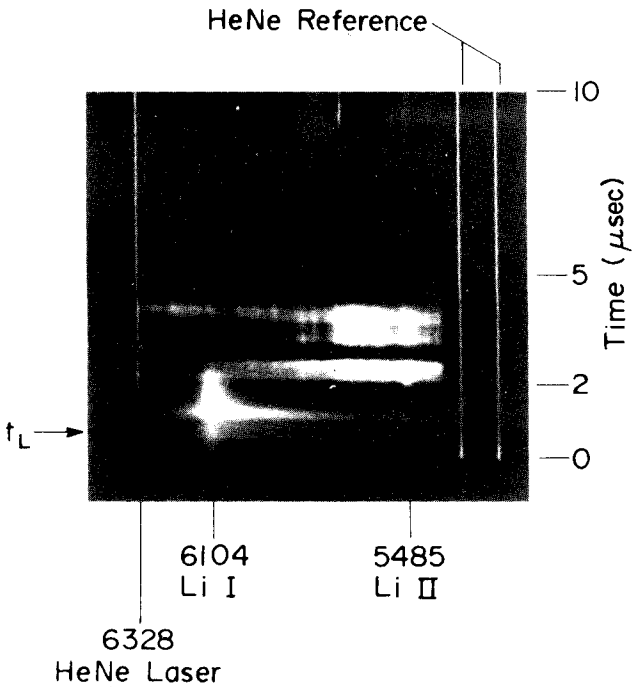

FIG. 12. Time-resolved spectra and the absorption of HeNe laser radiation.

in good agreement with a particle conservation calculation. The neutral IB absorption coefficient for 10.6-μ radiation was calculated from Eq. (3) to be 122 cm^{-1} and was a factor of 19 greater than the measured total absorption coefficient.

It was possible to explain the strong absorption at both wavelengths by assuming a spatial separation of the neutrals and the electrons in the plasma. A qualitative model of electron and neutral density distributions is illustrated in Fig. 13 and consists of a hot peripheral region predominantly containing electrons and single ionized lithium ions and a cold central region of excited neutrals.

The total absorption coefficient can be written

$$K_T \approx \frac{1}{D_p} \int_0^{D_p} [K_i^{IB}(r) + K_N^{IB}(r)]\, dl, \tag{9}$$

where D_p is the plasma diameter and dl is an element of path length of the laser beam through the plasma. In this model, ion IB absorption is dominant in the peripheral plasma region (i.e., $K_T \approx K_i^{IB}$ for large r) while neutral IB absorption is dominant in the central region of the plasma (i.e., $K_T \approx K_N^{IB}$ for small r). If we assume that K_N^{IB} (r small) $\approx K_i^{IB}$ (r large), then the total absorption coefficient is approximately the same for all r.

The electron density in the center of the plasma can be estimated and, as an example, consider the data listed as entry 12 in Table I. The average ion IB absorption coefficient was $K_i^{IB} = 6.48$ cm^{-1} and the measured neutral density was 3.6×10^{19} cm^{-3}. If we assume $K_N^{IB} = 6.48$ cm^{-1} and $\theta \approx 1$ eV in the central region of the plasma, then $N_e \approx 2.0\times10^{16}$ cm^{-3}.

Supporting evidence for the model was obtained by performing an absorption experiment with an exploded wire which was placed 1.5 mm off axis with respect to the spectrometer entrance slit. A typical streak picture of the plasma spectrum and 6328-Å laser line is shown in Fig. 14. The appearance of the emission spectrum was delayed by the time necessary for the perimeter of the plasma column to expand into the region imaged onto the spectrometer slit. An important observation was that strong 6328-Å absorption occurred later in time than the appearance of the 6104-Å neutral lithium line. Since the absorption of 6328-Å radiation was a direct measure of the neutral density, the delay in strong absorption indicated that the neutral density was larger toward the center of the discharge. When the wire was exploded on axis, no delays were observed. The plasma emission and 6328-Å absorption were observed to begin at the same time (Fig. 12).

A qualitative description of the temperature distribution was obtained from a one-dimensional magnetohydrodynamic computer code.[29] The electron temperatures at the plasma perimeter were found to be as high as 40 eV at about 2 μsec. Although the calculations accurately demonstrated the plasma pinching, the plasma diameters were always much larger than those observed. Thus the calculated temperature profile appeared to be more accurate than the magnitude. The plasma current skin depth was always much larger than the plasma diameter which indicated that the current penetrated well into the plasma. The distribution was an exponentially increasing function of plasma radius, with maximum current, and hence heating, at the plasma perimeter. This implied a temperature profile consistent with our qualitative model.

Although exploded wire plasmas with a cold central

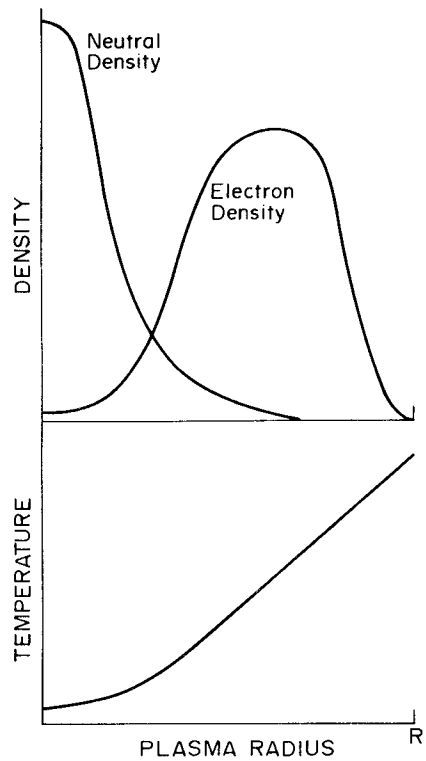

FIG. 13. Qualitative model for plasma specie and temperature distributions.

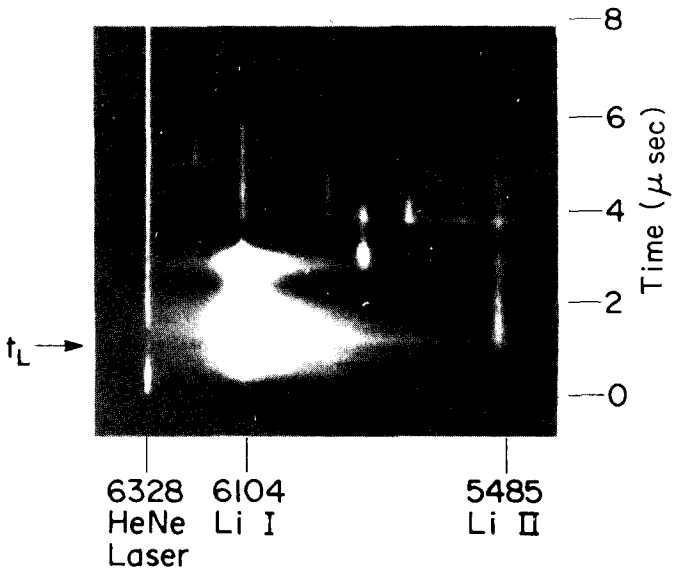

FIG. 14. Time-resolved spectra and the absorption of HeNe laser radiation for a plasma formed 1.5 mm off axis.

core and hotter outside region have been reported before,[30,31] the experimental parameters varied significantly from those in this investigation. We believe that this is the first evidence that such profiles exist for the first few microseconds for small-diameter wires exploded in high vacuum with a large discharge voltage.

V. SUMMARY

Absorption of laser radiation at two different wavelengths, 10.6 μ and 6328 Å, was observed in an exploded lithium wire plasma. In order to explain consistently the strong absorption of both laser wavelengths and the observed total absorption coefficient for 10.6-μ radiation, qualitative density and temperature profiles were developed. The plasma was believed to contain a cold central region of excited neutrals and a hotter peripheral region consisting of electrons and singly ionized lithium ions. Absorption of 10.6-μ radiation was dominated by ion inverse bremsstrahlung in the peripheral plasma region and by neutral inverse bremsstrahlung in the central region of the plasma.

The model was supported by computer calculations and spectroscopic observations. The individual specie contributions to the total absorption could be determined by a direct density profile measurement such as could be obtained by two-wavelength double-exposure holography.[32]

*Work supported in part by the Air Force Office of Scientific Research.
†Based in part upon a thesis submitted by J.C. DeBoo to the University of Michigan for which partial support was obtained from the National Science Foundation and the Consumers Power Company.
‡Present address: General Atomic Co., P.O. Box 81608, San Diego, Calif. 92138.
[1]F. Floux, Nucl. Fusion **11**, 635 (1971).
[2]J. Nuckolls, L. Wood, A. Thiessen, and G. Zimmerman, Nature (Lond.) **239**, 139 (1972).
[3]K. Brueckner, IEEE Trans. Plasma Sci. **PS-1**, 13 (1973).
[4]D.F. DuBois and M.V. Goldman, Phys. Rev. **164**, 207 (1967).
[5]A.A. Galeev and R.Z. Sagdeev, Nucl. Fusion **13**, 603 (1973).
[6]K. Nishikawa, J. Phys. Soc. Jpn. **24**, 916 (1968).
[7]V.P. Silin, Sov. Phys.-JETP **21**, 1127 (1965).
[8]J.L. Bobin, M. Decroisette, B. Meyer, and Y. Vitel, Phys. Rev. Lett. **30**, 594 (1973).
[9]K. Eidmann and R. Sigel, Max-Planck-Institut Fur Plasmaphysik, Lab. Report No. IPP IV/46, 1972 (unpublished).
[10]D.W. Forslund, J.M. Kindel, and E.L. Lindman, Phys. Rev. Lett. **30**, 739 (1973).
[11]M. Porkolab, V. Arunasalam, and R.A. Ellis, Jr., Phys. Rev. Lett. **29**, 1438 (1972).
[12]E. Oktay and D.R. Bach, J. Appl. Phys. **41**, 1716 (1970).
[13]K.W. Billman, J.R. Stallcop, P.D. Rowley, and L.L. Presley, Phys. Rev. Lett. **28**, 1435 (1972).
[14]D.L. Jassby, UCLA Plasma Engineering Laboratory Report No. UCLA-34P157, 1972 (unpublished).
[15]A.G. Englehardt, V. Fuchs, C.R. Neufeld, C. Richard, and R. Decoste, Appl. Phys. Lett. **20**, 425 (1972).
[16]J. Marrineau and H. Pepin, J. Appl. Phys. **43**, 917 (1972).
[17]M.F. Weisbach and H.G. Ahlstrom, Phys. Fluids **16**, 1164 (1973).
[18]T.A. Leonard and D.R. Bach, J. Appl. Phys. **44**, 2555 (1973).
[19]A.W. Weiss, Phys. Rev. **166**, 70 (1968).
[20]L. Spitzer, *Physics of Fully Ionized Gases* (Interscience, New York, 1962).
[21]W.S. Karzas and R. Latter, Astrophys. J. Suppl. Ser. **6**, 167 (1961—1962).
[22]H.S. Tsai, Z. Akcasu, and R.K. Osborn, University of Michigan, College of Engineering Technical Report No. 07599-18-T, 1968 (unpublished).
[23]H.S. Tsai, E. Oktay, and Z. Akcasu, J. Appl. Phys. **42**, 5469 (1972).
[24]H.R. Griem, *Plasma Spectroscopy* (McGraw-Hill, New York, 1964).
[25]C.B. Wheeler and S.J. Fielding, Plasma Phys. **12**, 551 (1970).
[26]A.F. Gibson, M.F. Kimmett, and A.C. Walker, Appl. Phys. Lett. **17**, 75 (1970).
[27]W.M. Doyle, Laser Focus **6**, 34 (1970).
[28]H.R. Griem, Phys. Rev. **165**, 258 (1968).
[29]D. Chapin, J.J. Duderstadt, and D.R. Bach, J. Appl. Phys. **45**, 1726 (1974).
[30]D.Y. Cheng, W.J. Loubsky, and V.E. Fousekis, Phys. Fluids **14**, 2328 (1971).
[31]W. Tiemann, Naturforsch. A **23**, 1952 (1969).
[32]R.A. Jeffries, Phys. Fluids **13**, 210 (1970).